Thermophysical Properties Measurements of Rocket Propellants RP-1 and RP-2

Stephanie L. Outcalt* and Arno Laesecke*
National Institute of Standards and Technology, Boulder, Colorado 80305-3328
and
Karin J. Brumback[†]
Yale University, New Haven, Connecticut 06520-8107

The density, speed of sound, and viscosity of two rocket propellants (RP-1 and RP-2) have been measured. Densities were measured with two different instruments. Data at ambient atmospheric pressure were obtained with a rapid characterization instrument from 278.15 to 343.15 K that measured the speed of sound and density of the liquids in parallel. Adiabatic compressibilities derived from that data are included here. Densities of the compressed liquids were measured in an automated apparatus from 270 to 470 K and pressures to 40 MPa. Viscosities of the two liquids were measured in an open gravitational capillary viscometer at ambient atmospheric pressure from 293.15 to 373.15 K. The measurement results are consistent with compositional differences between the two samples. Correlations have been developed to represent the measured properties within the estimated uncertainties of the experimental data and to allow physically meaningful extrapolations beyond the range of the measurements.

Nomenclature

C	=	viscometer calibration constant
E	=	viscometer calibration constant
p	=	pressure
p_{ref}	=	reference pressure, 0.083 MPa
T	=	temperature
T_r	=	reduced temperature, $T/273.15$ K
t	=	efflux time
V	=	volume
w	=	speed of sound
α_p	=	isobaric thermal expansivity
β_i	=	correlation coefficients
η	=	dynamic viscosity
κ_s	=	adiabatic compressibility at constant entropy
ρ	=	density
ν	=	kinematic viscosity

Introduction

EQUATIONS of state that accurately predict thermodynamic properties of fluids are often used to aid in the design of combustion machinery. These types of equations are the backbone of fluid properties databases such as the National Institute of Standards and Technology (NIST) software Reference Fluid Thermodynamic and Transport Properties (REFPROP) [1]. The formulation of accurate equations of state requires accurate thermophysical property data, in particular density and speed of sound over wide ranges of temperature and pressure. This is especially true when working with complex mixtures. Such data are presented here for the two rocket propellants RP-1 and RP-2. They were obtained using three different instruments to measure density, speed of sound, and viscosity at atmospheric pressure, and compressed liquid density in the combined range from 270 to 470 K with pressures to 40 MPa.

The measurements reported here were part of a larger effort at NIST to characterize two hydrocarbon rocket propellants, RP-1 and RP-2. The studies were undertaken to provide the United States Air Force with the information and tools necessary to design new rocket propellants that would facilitate the ability to use rocket motors multiple times. This requirement dictates that the fuel be very low in sulfur components, aromatics, and alkenes. RP-1 is considered the traditional hydrocarbon rocket propellant, and is a kerosenelike, complex mixture which typically includes linear and branched paraffins, alkenes, and aromatics [2,3]. The RP-2 sample studied in this work was a reformulated grade of hydrocarbon rocket propellant. Properties investigated in this effort included distillation curves, thermal decomposition products, and thermophysical equilibrium and transport properties. These measurements facilitated the correlation of equations of state for each of the fluids, the ultimate tool to aid in efficient and effective design of advanced rocket engines.

Test Samples

RP-1 and RP-2 samples were provided by the Fuels Branch of the United States Air Force Research Laboratory, Wright-Patterson Air Force Base, Ohio. Their compositions were analyzed at NIST with a gas chromatography, mass spectrometry, infrared spectrometry method [3], and compounds having chromatographic peak area counts in excess of 1% were reported. The differences between the two samples can be summarized as follows: the RP-1 sample contained alkanes up to C14 (methyltridecane isomers) and approximately 1% (peak area) aromatic hydrocarbons (1-methylnaphthalene), whereas the RP-2 sample contained alkanes up to C_{16} (hexadecane) and no reported aromatic hydrocarbons. Other major differences between the RP-1 and RP-2 samples include the fact that RP-2 contained less sulfur, whereas RP-1 contained a pink dye additive.

The composition of the RP-1 sample was detailed in the publication of Bruno and Smith [3]. The critical temperatures of the RP-1 constituents as listed in the NIST Chemistry WebBook [4] range from 639 K for n-undecane to 772 K for 1-methylnaphthalene. This temperature range provides a rough estimate for the critical temperature of the RP-1 mixture.

The composition of the RP-2 sample is specified in the report of Ott et al. [5]. The content of different aromatic compounds and the higher content of alkanes in RP-2 results in a significantly different upper limit of the critical temperature and is given by the critical temperature of hexadecane at 722 K. Thus, a lower critical temperature is expected for RP-2 than for RP-1. The RP-2 sample contained a significantly higher fraction of larger alkane molecules

*Chemical Engineer, NIST Mail Stop 838.07.
[†]Graduate Student, Department of Chemistry.

Table 1   Measured density, speed of sound, and calculated adiabatic compressibility of samples of RP-1 and RP-2 measured in the density and sound speed analyzer DSA 5000[a]

	RP-1 sample				RP-2 sample		
Temperature, K	Density ρ, kg $\cdot$ m^{-3}	Speed of sound w, m $\cdot$ s^{-1}	Adiabatic compressibility κ_s, TPa^{-1}	Temperature, K	Density ρ, kg $\cdot$ m^{-3}	Speed of sound w, m $\cdot$ s^{-1}	Adiabatic compressibility κ_s, TPa^{-1}
278.15	815.50	1381.3	642.67	278.15	817.10	1383.3	639.19
283.15	811.86	1361.2	664.77	283.15	813.48	1363.6	661.14
293.15	804.59	1321.7	711.49	293.15	806.23	1324.1	707.51
303.15	797.33	1283.0	761.97	303.15	798.93	1285.3	757.62
313.15	790.05	1245.0	816.62	313.15	791.67	1247.4	811.76
323.15	782.76	1207.7	875.89	323.15	784.41	1210.3	870.36
333.15	775.44	1171.1	940.33	333.15	777.07	1173.8	933.98
343.15	768.09	1135.6	1009.7	343.15	769.80	1138.2	1002.8

[a]The ambient atmospheric pressure during the measurements was 0.083 MPa corresponding to an altitude of 1633 m above sea level at Boulder, Colorado.

than RP-1, which would result in a higher viscosity, especially at low temperatures, because this property is most sensitive to molecular size, shape, and charge distribution (polarity) that give rise to attractive and repulsive forces between molecules. Because of the complexity of the two mixtures, it is more difficult to anticipate how their composition influences their density and speed of sound.

Experimental

Two apparatus were used to perform the density measurements presented here. Both instruments employ vibrating-tube sensors. Their calibration and operating procedures have been described previously in the context of measurements of methyl- and propylcyclohexane [6]. A density and sound speed analyzer DSA 5000, Anton–Paar Corporation,[‡] was used to determine these properties at atmospheric pressure (0.083 MPa at the altitude of Boulder, Colorado). Temperature scans were programmed in the units of the instrument from 70°C to 10°C in decrements of 10°C followed by a single measurement at 5°C. Densities of the test liquids were measured during the same temperature scans that were carried out to obtain their speeds of sound. The relative standard deviation of the repeated density measurements was lower than 0.003%, and the manufacturer quoted uncertainty is 0.1% for both density and speed of sound. Compressed liquid density measurements were made with the fully automated densimeter of Outcalt and McLinden [7] over the temperature range of 270 to 470 K, and up to pressures of 40 MPa. The densimeter is calibrated with propane and toluene and the expanded uncertainty in density is calculated to be 0.64 kg $\cdot$ m^{-3} to 0.81 kg $\cdot$ m^{-3} (coverage factor $k = 2$) [8].

Viscosity measurements were carried out at atmospheric pressure in the temperature range 293.15 to 373.15 K. The instrument used was an automated open gravitational flow viscometer with a suspended level Ubbelohde glass capillary of 200 mm length with upper reservoir bulbs for a kinematic viscosity range from 0.3 mm^2 $\cdot$ s^{-1} to 30 mm^2 $\cdot$ s^{-1} (miniAV, Cannon Instrument Company). The glass capillary is mounted in a thermostatting bath filled with silicone oil. The thermostat includes a stirrer, a heat pipe to a thermoelectric Peltier cooler at the top of the instrument, and a 100 Ω platinum resistance temperature probe (PRT) that is read with an alternating current resistance bridge (F250, Automatic Systems Laboratories). The bath temperature is set with the operating software that is an integral part of the viscosity measurement system, and it is controlled within ±0.02 K between 293.15 K and 373.15 K. The calibration of the PRT on the International Temperature Scale of 1990 was verified by comparison with a water triple point cell. The estimated uncertainty of the temperature measurement system is 0.02 K.

The capillary viscometer system allows viscosity measurements relative to liquids with accurately known viscosities. Calibrations were performed with certified viscosity standards N.4, N1.0, S3, and S6 obtained from the Cannon Instrument Company to determine the constants C and E of the working equation

$$\nu = (C \cdot t) - E/t^2$$

The first term on the right hand side of this equation is the reformulated Hagen–Poiseuille expression for gravitational laminar flow in a circular tube, whereas the second term is the Hagenbach correction for kinetic energy losses. The symbol ν denotes the kinematic viscosity (momentum diffusivity) in mm^2 $\cdot$ s^{-1} and t is the efflux time in seconds of a known volume of liquid flowing through the capillary. Efflux times are measured with three thermistor sensors on the outside of the capillary above, in between, and below the two measuring bulbs. The thermistors detect the passing of the liquid meniscus at their locations and trigger an internal stopwatch. Depending on the viscosity range the upper or middle thermistors are used to time the efflux of the test liquid through the respective measuring bulb of known volume.

The viscosity measurement system includes components to pump the test liquid into the upper measuring bulbs for repetitive efflux timings and to flush the capillary tube with two different solvents (hexanes and acetone) when the test liquid is changed. The operating software was set to perform up to five measurements until three
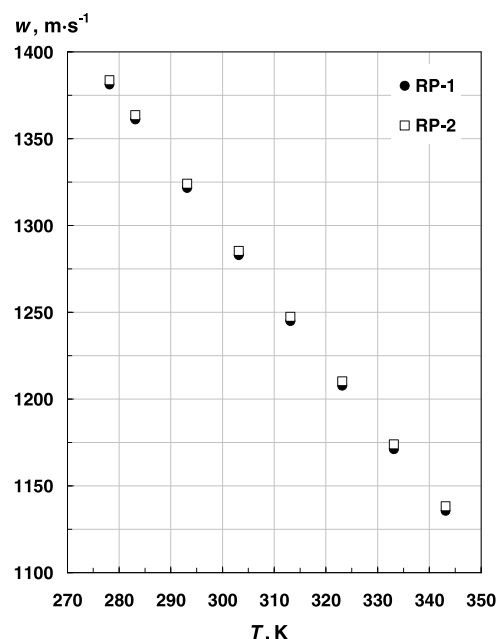
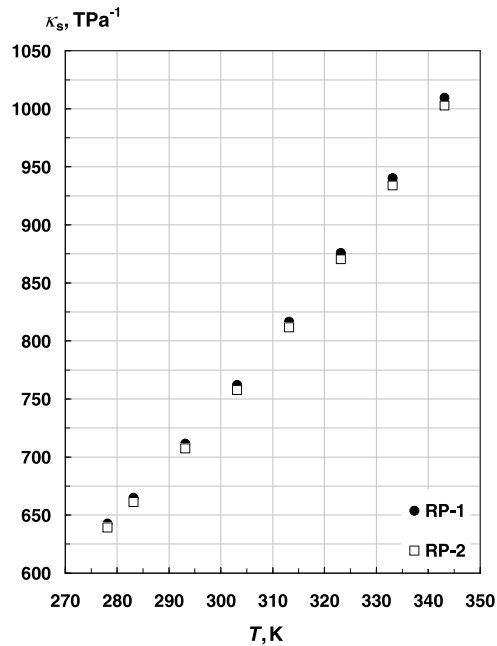**Fig. 1   Measured speed of sound data of RP-1 and RP-2 as a function of temperature at ambient pressure.**

Fig. 2 Calculated adiabatic compressibility of RP-1 and RP-2 as a function of temperature at ambient pressure.

agreed within 0.5% repeatability. The three runs were averaged to calculate the viscosity. The expanded uncertainty [8] of the viscosity data reported here is estimated to be 1.5% (coverage factor $k = 2$) to account for variations in the constants C and E that occurred for calibrations with different viscosity standards and to a lesser degree for calibrations at different temperatures.

The design of the instrument, its calibration, and operation conform to the ASTM International (ASTM) standards D445, D446, and D2162 [9–11], and the corresponding ISO standards 3104 and 3105 [12,13].

Results

Table 1 lists values of density, speed of sound, and derived adiabatic compressibilities for RP-1 and RP-2 at ambient pressure from 278.15 to 343.15 K. Adiabatic compressibilities were calculated from the measured densities and speeds of sound via the thermodynamic relation

$$\kappa_s = -(\partial V/\partial p)_s/V = 1/(\rho w^2) \qquad (1)$$

where V denotes volume, p is pressure, ρ is the density, and w the speed of sound. The subscript s indicates "at constant entropy." The data for the speed of sound and adiabatic compressibility are depicted in Figs. 1 and 2, respectively. It can be concluded from Table 1 and Figs. 1 and 2 that the two fluids have very similar thermodynamic properties at atmospheric pressure.

Table 2 Density of a sample of RP-1 measured in the high-pressure vibrating-tube densimeter along isotherms from 270 to 470 K in increments of 20 K[a]

270 K		290 K		310 K		330 K		350 K		370 K
Pressure p, MPa	Density ρ, kg·m^{-3}	Pressure p, MPa	Density ρ, kg·m^{-3}	Pressure p, MPa	Density ρ, kg·m^{-3}	Pressure p, MPa	Density ρ, kg·m^{-3}	Pressure p, MPa	Density ρ, kg·m^{-3}	Pressure p, MPa
40.00	843.2	40.00	831.1	40.00	818.7	39.99	806.3	39.99	794.3	40.00
35.00	840.8	35.00	828.5	34.99	815.9	35.00	803.2	35.02	791.0	35.00
30.01	838.3	30.00	825.8	29.99	812.9	30.00	800.0	30.00	787.5	30.00
25.01	835.8	25.00	823.0	25.00	809.8	25.00	796.7	24.99	784.0	24.99
20.00	833.2	20.01	820.1	20.01	806.6	19.99	793.3	20.00	780.2	20.00
15.00	830.5	15.01	817.2	14.99	803.3	15.00	789.7	14.99	776.3	15.01
10.00	827.7	9.99	814.1	10.00	799.9	10.00	785.9	10.01	772.2	10.00
5.00	824.8	5.02	810.9	4.99	796.3	5.00	782.0	5.00	767.8	4.99
4.00	824.2	4.00	810.2	4.00	795.6	3.99	781.2	4.00	766.9	4.00
3.00	823.6	3.00	809.6	3.00	794.8	3.00	780.4	3.01	766.0	3.00
2.00	823.0	1.99	808.9	2.00	794.1	2.00	779.5	2.00	765.1	2.00
1.00	822.4	1.00	808.2	0.99	793.3	1.00	778.7	0.99	764.1	1.00
0.50	822.1	0.49	807.9	0.50	792.9	0.50	778.3	0.50	763.7	0.50
0.083	*821.9*	*0.083*	*807.6*	*0.083*	*792.6*	*0.083*	*777.9*	*0.083*	*763.3*	*0.083*

370 K	390 K		410 K		430 K		450 K		470 K	
Density ρ, kg·m^{-3}	Pressure p, MPa	Density ρ, kg·m^{-3}	Pressure p, MPa	Density ρ, kg·m^{-3}	Pressure p, MPa	Density ρ, kg·m^{-3}	Pressure p, MPa	Density ρ, kg·m^{-3}	Pressure p, MPa	Density ρ, kg·m^{-3}
782.5	40.01	770.7	40.03	759.0	39.99	747.3	40.00	735.7	40.00	724.3
778.9	35.00	766.9	35.00	754.9	35.00	742.9	35.00	731.0	35.00	719.2
775.2	30.01	762.9	30.00	750.6	30.00	738.2	30.00	725.9	30.00	713.7
771.3	25.00	758.7	25.00	746.0	24.99	733.2	25.00	720.5	25.00	707.8
767.2	20.00	754.2	20.00	741.1	20.00	727.9	20.01	714.7	20.00	701.5
763.0	15.00	749.5	15.01	735.9	15.00	722.2	14.99	708.4	14.99	694.5
758.4	10.01	744.4	10.01	730.4	9.99	716.0	10.01	701.5	10.01	686.8
753.6	5.01	739.0	5.01	724.3	5.01	709.2	5.00	693.7	5.00	678.0
752.5	4.00	737.9	4.01	723.0	4.00	707.7	4.00	692.0	4.01	676.1
751.5	3.00	736.7	3.00	721.7	3.00	706.2	3.00	690.3	3.00	674.1
750.5	2.00	735.5	2.00	720.3	2.00	704.7	2.00	688.6	1.99	672.1
749.4	1.00	734.3	1.01	719.0	1.00	703.1	1.00	686.8	0.99	670.0
748.9	0.51	733.7	0.50	718.3	0.49	702.3	0.50	685.8	0.50	668.9
748.4	*0.083*	*733.2*	*0.083*	*717.7*	*0.083*	*701.6*	*0.083*	*685.1*	*0.083*	*668.0*

[a]Values extrapolated to 0.083 MPa are indicated in *italics*.

Table 3   Density of a sample of RP-2 measured in the high-pressure vibrating-tube densimeter along isotherms from 270 to 470 K in increments of 20 K[a]

270 K		290 K		310 K		330 K		350 K		370 K
Pressure p, MPa	Density ρ, kg·m⁻³	Pressure p, MPa	Density ρ, kg·m⁻³	Pressure p, MPa	Density ρ, kg·m⁻³	Pressure p, MPa	Density ρ, kg·m⁻³	Pressure p, MPa	Density ρ, kg·m⁻³	Pressure p, MPa
39.97	844.0	39.98	832.0	39.99	819.9	39.98	807.7	40.01	795.7	39.99
34.99	841.5	35.00	829.5	35.00	817.0	34.99	804.6	35.00	792.4	35.01
30.00	839.1	29.99	826.8	29.99	814.0	30.00	801.4	30.00	789.0	30.00
25.01	836.6	25.00	824.0	25.00	810.9	25.00	798.2	25.00	785.4	25.00
20.00	833.9	20.00	821.2	20.00	807.7	19.99	794.7	20.00	781.7	20.00
15.00	831.2	14.99	818.2	15.01	804.5	15.00	791.2	14.99	777.8	15.00
10.00	828.4	10.00	815.2	10.00	801.0	10.00	787.5	10.00	773.7	10.00
5.00	825.6	5.00	812.0	4.99	797.5	5.00	783.5	4.99	769.4	5.00
4.00	825.0	3.99	811.3	4.00	796.8	3.99	782.7	3.99	768.4	3.99
3.00	824.4	3.00	810.7	3.00	796.0	2.99	781.9	3.00	767.5	2.99
2.00	823.8	2.00	810.0	1.99	795.3	2.00	781.1	2.00	766.6	2.00
1.00	823.2	1.00	809.3	1.00	794.5	1.00	780.2	0.99	765.7	1.00
0.49	822.9	0.50	809.0	0.50	794.2	0.49	779.8	0.50	765.2	0.50
0.083	*822.6*	*0.083*	*808.7*	*0.083*	*793.8*	*0.083*	*779.4*	*0.083*	*764.8*	*0.083*

370 K	390 K		410 K		430 K		450 K		470 K	
Density ρ, kg·m⁻³	Pressure p, MPa	Density ρ, kg·m⁻³	Pressure p, MPa	Density ρ, kg·m⁻³	Pressure p, MPa	Density ρ, kg·m⁻³	Pressure p, MPa	Density ρ, kg·m⁻³	Pressure p, MPa	Density ρ, kg·m⁻³
783.9	39.98	772.2	39.99	760.5	40.00	748.9	40.02	737.4	39.96	726.0
780.3	35.00	768.4	35.00	756.4	34.99	744.5	34.99	732.6	35.00	721.0
776.7	30.00	764.4	30.00	752.1	30.01	739.9	30.00	727.6	30.00	715.5
772.8	25.01	760.2	24.99	747.6	25.00	734.9	25.01	722.2	25.00	709.7
768.8	19.99	755.8	20.00	742.8	20.01	729.6	20.02	716.4	19.99	703.3
764.5	14.99	751.1	15.00	737.6	14.99	723.9	15.00	710.1	15.00	696.4
760.0	10.00	746.1	10.00	732.1	10.01	717.8	10.00	703.2	10.01	688.8
755.2	5.00	740.7	4.99	726.0	4.99	710.9	5.00	695.6	5.01	680.1
754.1	4.00	739.5	4.00	724.7	4.00	709.5	3.99	693.9	4.00	678.2
753.1	3.00	738.4	3.00	723.4	3.00	708.0	3.00	692.2	2.99	676.2
752.1	2.00	737.2	2.00	722.1	1.99	706.5	2.00	690.5	1.99	674.2
751.0	0.99	736.0	0.99	720.7	1.00	704.9	1.00	688.7	1.00	672.2
750.5	0.50	735.4	0.50	720.0	0.50	704.1	0.50	687.8	0.49	671.1
750.0	*0.083*	*734.9*	*0.083*	*719.5*	*0.083*	*703.5*	*0.083*	*687.0*	*0.083*	*670.2*

[a]Values extrapolated to 0.083 MPa are indicated in *italics*.

Listed in Tables 2 and 3 are measured values of compressed liquid density from 270 to 470 K to pressures of 40 MPa for RP-1 and RP-2, respectively. Also listed are density values extrapolated to 0.083 MPa for each temperature. These were obtained by fitting a second order polynomial to the isothermal data at pressures less than or equal to 10 MPa and extrapolating to 0.083 MPa. This extrapolation was performed to examine the consistency of the compressed liquid data with the measurement results at ambient pressure from the density and sound speed analyzer. Agreement between the data sets can be examined visually in Figs. 3 (RP-1) and 4 (RP-2). In the next section an analytical comparison of the two sets of density data is presented.

Table 4 lists both the measured kinematic and derived dynamic viscosity data from 293.15 to 373.15 K at ambient pressure for RP-1 and RP-2. Dynamic or absolute viscosities were calculated from the measured kinematic viscosities according to $\eta = \nu \cdot \rho$ by use of the correlation of the density data at atmospheric pressure, Eq. (3), that is described in the next section. These kinematic viscosity data are also represented graphically in Fig. 5. It should be noted that of the properties reported here, the viscosity values exhibit the greatest difference between the two fuels. The viscosities of RP-1 are between 3 and 5% lower than those of RP-2 at the same temperatures, whereas their density, speed of sound, and adiabatic compressibility values differ by less than 1%. It is well known that viscosity reflects differences in molecular size, shape, and charge distribution with much greater resolution than other thermophysical properties. The differences between the two samples that were detected in the viscosity measurements are consistent with the significantly higher fraction of larger alkane molecules in RP-2 than in RP-1, and are detailed in the Test Samples section of this paper.
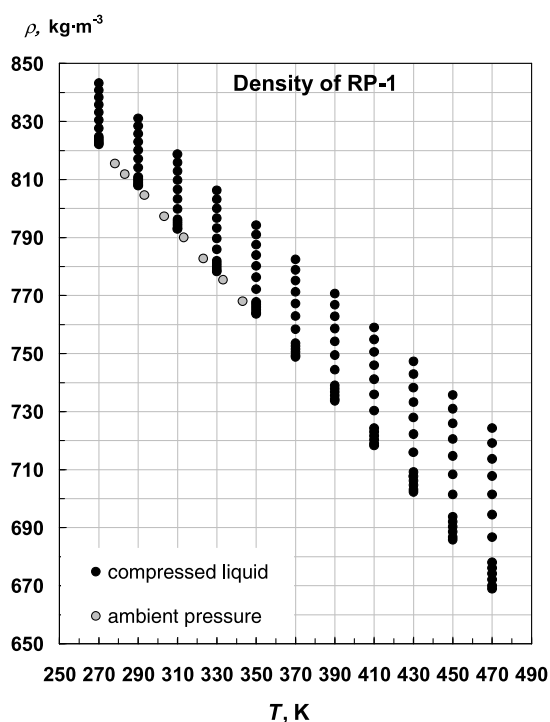
Fig. 3   Measured density data of RP-1 as a function of temperature with pressures up to 40 MPa. Along isotherms of compressed liquid data, the highest density corresponds to 40 MPa and lowest to 0.5 MPa.
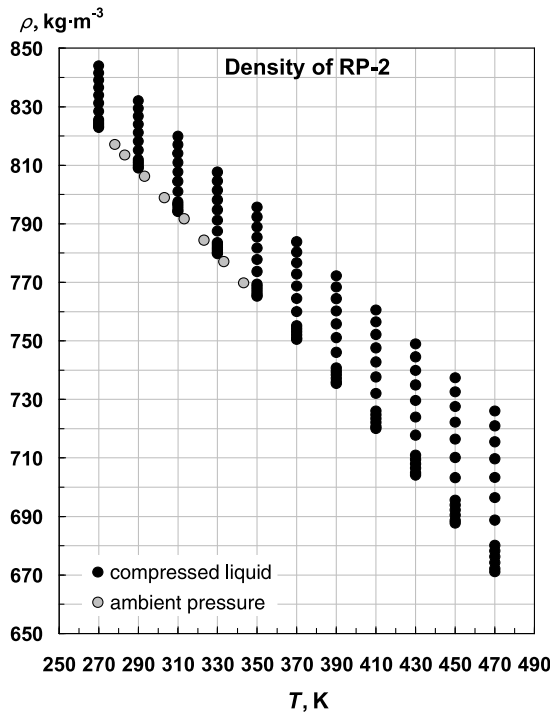
Fig. 4 Measured density data of RP-2 as a function of temperature with pressures up to 40 MPa. Along isotherms of compressed liquid data, the highest density corresponds to 40 MPa and lowest to 0.5 MPa.

Fig. 5 Measured kinematic viscosities of RP-1 and RP-2 as a function of temperature at ambient pressure.

Data Correlation

An informed choice of functional forms for data correlations can significantly enhance the value of experimental results and make them useful beyond the range of measurements [14]. Here, correlations are employed that represent the measurement results within their estimated uncertainty and can be extrapolated reliably beyond the measured temperature range. Because of the variability in samples of rocket propellants, it should be noted that the correlations provided here are specific to the samples studied in this work and should not be generically applied to hydrocarbon rocket propellants, nor should the extrapolations be applied when there is reasonable likelihood of chemical restructuring (e.g., cracking) that would significantly change the composition of the fluid.

Speed of Sound and Density

Until recently, the speed of sound of liquids was not often measured at atmospheric pressure because such instruments were not widely available. Consequently, there are no well-established correlating equations to represent such speed of sound data. Figure 1 suggests that the temperature dependence of the measured speed of sound data of the two rocket propellant samples is linear. However, a straight-line fit in temperature turned out to be insufficient to
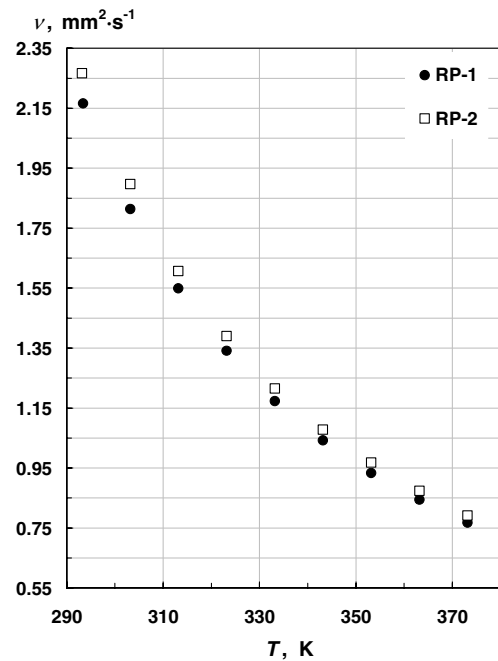
represent the data within their expanded uncertainty. A quadratic polynomial in absolute temperature T,

$$w = \beta_1 + \beta_2 \cdot T + \beta_3 \cdot T^2 \qquad (2)$$

accomplished such data representation. Values of the adjustable parameters β_1 to β_3 and regression statistics are listed in Table 5 for both RP-1 and RP-2. The extrapolation behavior of the polynomials was examined up to 470 K and was found to be reasonable.

Densities of liquids at atmospheric pressure have been measured far more often than the corresponding speeds of sound. Therefore, well-established correlating equations have emerged that represent such density data over wide temperature ranges and extrapolate to physically meaningful values beyond the temperature range of experimental data. One such formulation is the Rackett equation,

$$\rho(T) = \beta_4 \cdot \beta_5^{-(1+(1-T/\beta_6)^{\beta_7})} \qquad (3)$$

where the parameter β_6 is normally constrained to the critical temperature. Since the critical temperatures of the rocket propellants have not yet been determined, the parameter β_6 was included in the nonlinear regression. The pressure and temperature dependences of the compressed liquid density data were correlated with the Tait equation,

Table 4 Kinematic viscosity of samples of RP-1 and RP-2 measured in the open gravitational capillary viscometer system[a]

	RP-1 sample			RP-2 sample	
Temperature T, K	Kinematic viscosity ν, $\mathrm{mm^2 \cdot s^{-1}}$	Dynamic viscosity η, $\mathrm{mPa \cdot s}$	Temperature T, K	Kinematic viscosity ν, $\mathrm{mm^2 \cdot s^{-1}}$	Dynamic viscosity η, $\mathrm{mPa \cdot s}$
373.15	0.7678	0.5727	373.16	0.7916	0.5918
363.15	0.8445	0.6362	363.15	0.8735	0.6595
353.15	0.9335	0.7103	353.15	0.9683	0.7383
343.15	1.042	0.8007	343.15	1.078	0.8298
333.15	1.173	0.9100	333.15	1.215	0.9446
323.18	1.341	1.050	323.15	1.390	1.091
313.12	1.549	1.225	313.15	1.607	1.272
303.18	1.814	1.447	303.15	1.897	1.516
293.38	2.166	1.743	293.15	2.267	1.828

[a]The ambient atmospheric pressure during the measurements was 0.083 MPa corresponding to an altitude of 1633 m above sea level at Boulder, Colorado.

Table 5 Parameters of the correlations for the speed of sound, Eq. (1), of RP-1 and RP-2 at ambient atmospheric pressure and temperatures from 278.15 to 343.15 K[a]

Equation 5	RP-1 sample		RP -2 sample	
Parameters	Value	Standard deviation	Value	Standard deviation
$\beta_1/(\text{m} \cdot \text{s}^{-1})$	2797.7044	6.2	2809.8695	6.1
$\beta_2/(\text{m} \cdot \text{s}^{-1} \cdot \text{K}^{-1})$	−6.1546685	0.040	−6.2215696	0.039
$\beta_3/(\text{m} \cdot \text{s}^{-1} \cdot \text{K}^{-2})$	$3.8195817 \cdot 10^{-3}$	$6.5 \cdot 10^{-5}$	$3.9342693 \cdot 10^{-3}$	$6.4 \cdot 10^{-5}$
AAD, %	——	$3.9 \cdot 10^{-3}$	——	$2.9 \cdot 10^{-3}$
RMS, %	——	$4.9 \cdot 10^{-3}$	——	$3.3 \cdot 10^{-3}$

[a]Average absolute deviations (AAD) and root mean square deviations are given in percents to indicate the goodness of the correlations.

Table 6 Parameters of the Rackett correlations for the density, Eq. (3), of RP-1 and RP-2 at ambient atmospheric pressure and temperatures from 270 to 470 K
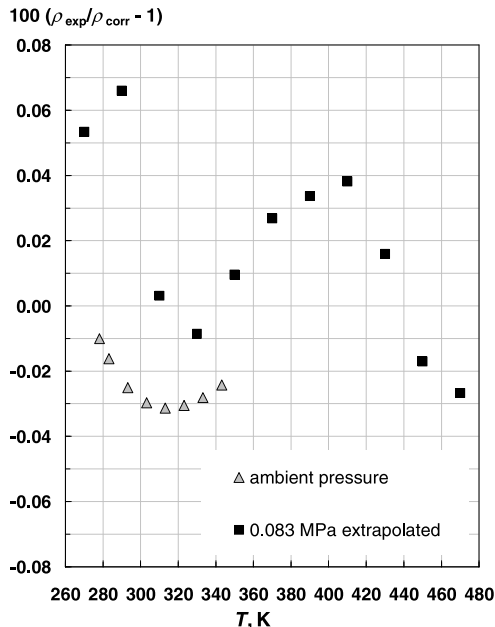
Equation 3	RP-1 sample		RP-2 sample	
Parameter	Value	Standard deviation	Value	Standard deviation
$\beta_4/(\text{kg} \cdot \text{m}^{-3})$	287.671 29	0.096	288.125 29	0.054
β_5	0.533 650 16	$8.7 \cdot 10^{-5}$	0.534 122 56	$4.9 \cdot 10^{-5}$
β_6/K	574.262 84	0.064	575.460 86	0.036
β_7	0.628 866 40	$1.3 \cdot 10^{-4}$	0.625 144 41	$7.2 \cdot 10^{-5}$

Table 7 Parameters of the Tait correlations, Eq. (4) and (5), for the density of RP-1 and RP-2 in terms of temperature and pressure

Equation	RP-1 sample		RP-2 sample	
Parameters	Value	Standard deviation	Value	Standard deviation
β_8/MPa	$79.635\,78 \cdot 10^{-3}$	$1.1 \cdot 10^{-4}$	$79.820\,30 \cdot 10^{-3}$	$9.6 \cdot 10^{-5}$
β_9/MPa	320.026 84	0.58	335.230 86	0.51
β_{10}/MPa	−285.519 55	0.61	−302.829 84	0.53
C	66.068 79	0.18	71.118 09	0.15

$$\rho(T, p) = \rho_{\text{ref}}(T, p_{\text{ref}}) \bigg/ 1 - C \ell_n \left(\frac{p + B(T)}{p_{\text{ref}} + B(T)} \right) \qquad (4)$$

where $\rho_{\text{ref}}(T)$ is the temperature-dependent density at the reference pressure $p_{\text{ref}} = 0.083$ MPa from Eq. (3), and C is a constant. The temperature dependence of the Tait parameter $B(T)$ was expressed by a quadratic polynomial,

$$B(T) = \beta_8 + \beta_9 \cdot T_r + \beta_{10} \cdot T_r^2 \qquad (5)$$

where T_r is the absolute temperature T divided by 273.15 K. Parameters and statistics for the Rackett correlations are listed in Table 6 and those for the Tait correlations in Table 7.

Figures 6 and 7 illustrate deviations of the experimental data from the Rackett correlations for RP-1 and RP-2, respectively. In both figures, our high-pressure data extrapolated to 0.083 MPa, and the ambient pressure data show agreement within the estimated experimental uncertainty of 0.1% of the high-pressure data. Figures 8 and 9 illustrate the deviations of all experimental density data from the Tait correlations for RP-1 and RP-2. The RP-1 data are fit to within 0.07% by the Tait correlation, and the RP-2 densities to within 0.05%. The Tait equation of state is known for its reliable extrapolation behavior to considerably higher pressures than those measured. In our previous study of methyl- and propylcyclohexane [6] it was found that the Tait equation based on our measurements up to pressures of 40 MPa represented literature data up to 100 MPa within their experimental uncertainty of 0.1%. If higher uncertainty is acceptable, the Tait equation of state can be extrapolated to substantially higher pressures, however, extrapolation beyond ±20 K of the temperature range of our measured data would not be recommended.

Figures 10 and 11 illustrate the isobaric thermal expansivity, α_p along isotherms as a function of pressure for RP-1 and RP-2, respectively. The isobaric thermal expansivity coefficients were obtained analytically by differentiating the Tait equation (4) according to the thermodynamic relation

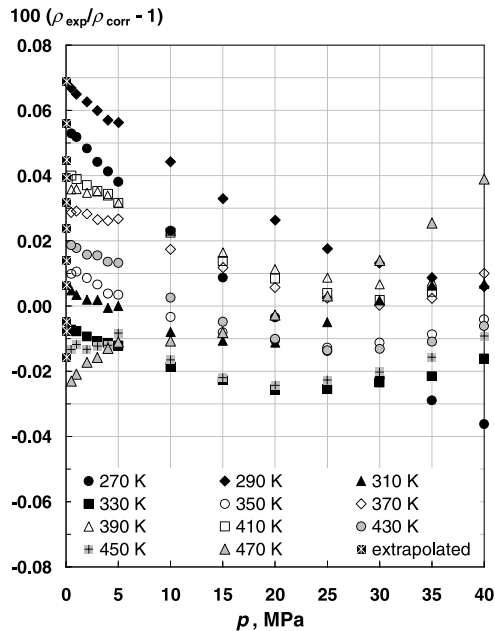**Fig. 6 Deviations of density data of RP-1 at ambient pressure from the Rackett correlation, Eq. (3).**
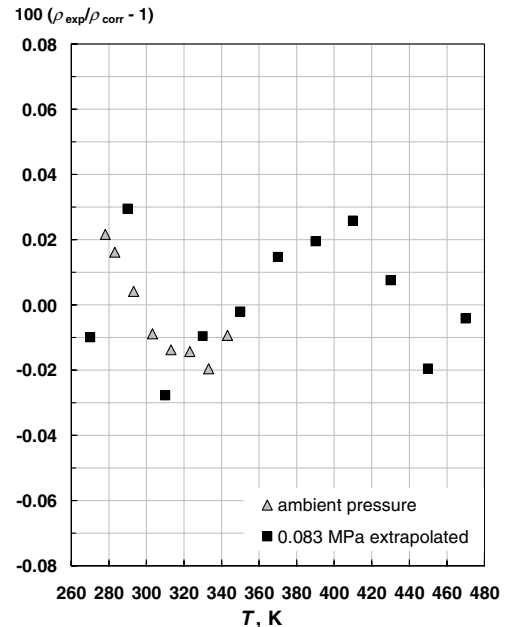
Fig. 7 Deviations of density data of RP-2 at ambient pressure from the Rackett correlation, Eq. (3).

Fig. 8   Deviations of all measured density data of RP-1 from the modified Tait correlation, Eq. (4).

Fig. 10   Isobaric thermal expansivity of RP-1 as function of temperature and pressure.

$$\alpha_p = -(1/\rho)(\partial\rho/\partial T)_p \qquad (6)$$

Many studies have shown that the isobaric thermal expansivities of pure liquids exhibit certain pressures where their isotherms cross and where the isobaric thermal expansivity does not depend on temperature [15]. This feature can be seen in Figs. 10 and 11 for both fuels at approximately 70 MPa, although it appears that it may be at a slightly lower pressure for RP-2. However, only the isotherms from 270 to 390 K intersect at this point, whereas crossovers of higher isotherms move to higher pressures.

Viscosity

A dual approach was taken to correlate the viscosity data at atmospheric pressure within their experimental uncertainty and with reliable extrapolation behavior. The combination of these two objectives is more difficult to fulfill for viscosity than for the other
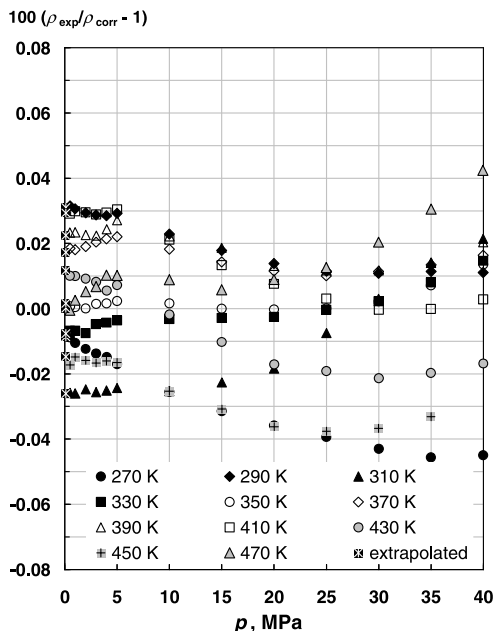
measured properties. The industrial importance of an accurate knowledge of viscosity–temperature dependences of liquids and their reliable extrapolation is signified by ASTM D341 [16].

A large number of empirically extended functional forms have been tried for representing viscosities of liquids over wide temperature ranges [17]. To represent the steep rise of viscosity with decreasing temperature, Vogel [18], Fulcher [19], and Tammann and Hesse [20] modified the original Arrhenius exponential in inverse temperature that arises from kinetic theories of liquids by an additional parameter, here denoted β_{12}:

$$\frac{\nu(T)}{\nu_0} = \exp\left(\frac{\beta_{11}}{T_r - \beta_{12}} + \beta_{13}\right) \qquad (7)$$

which marks a hypothetical temperature where the viscosity becomes infinite. T_r is the absolute temperature T divided by 273.15 K. This Vogel–Fulcher–Tammann (VFT) correlation is

Fig. 9   Deviations of all measured density data of RP-2 from the modified Tait correlation, Eq. (4).

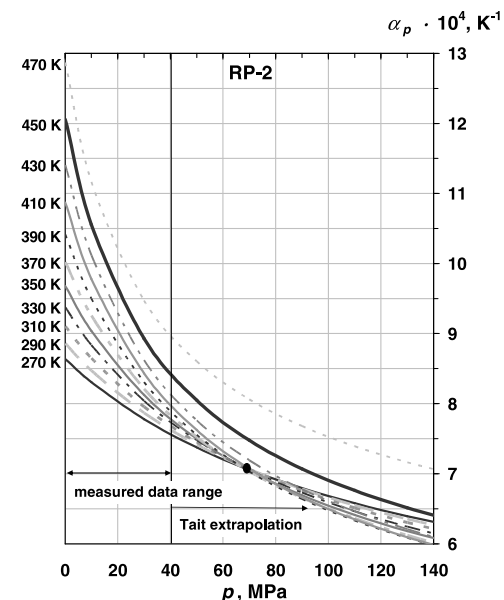Fig. 11   Isobaric thermal expansivity of RP-2 as function of temperature and pressure.

written here in terms of kinematic viscosity (momentum diffusivity) ν with the dimensioning factor ν_0, but it is equally applicable to the dynamic or absolute viscosity $\eta = \nu \cdot \rho$. At temperatures above the singularity marked by β_{12}, Eq. (7) represents a hyperbola whose curvature does not change sign. This feature limits the range of applicability of the VFT correlation towards higher temperatures because the viscosity of liquids does exhibit inflection points in that region. Therefore, systematically too high viscosities are obtained when VFT correlations based on data at low temperatures are extrapolated to temperatures above those that were measured.

One form that is successfully applied to a multitude of compounds in the Design Institute for Physical Properties (DIPPR) Project [21] and in the NIST ThermoData Engine [22] contains two temperature terms in addition to the original exponential in inverse temperature, and five adjustable parameters:

$$\frac{\nu(T)}{\nu_0} = \exp\left(\beta_{14} + \frac{\beta_{15}}{T_r} + \beta_{16}\, \ell_n(T_r) + \beta_{17} T_r^{\beta_{18}}\right) \qquad (8)$$

This correlation is capable of representing an inflection of the viscosity–temperature dependence at higher temperatures, while the power law term amplifies the inverse temperature exponential to capture the steep increase of viscosity at low temperatures.

The viscosity data for RP-1 and RP-2 in Table 4, measured from 293.15 to 373.15 K, were correlated well within their estimated experimental uncertainties with both forms, the VFT equation in Eq. (7), as well as Eq. (8). Root mean square (RMS) deviations with the VFT equation in Eq. (7) are 0.104% for the RP-1 data and 0.19% for the RP-2 data. Equation (8) represents the data with root mean square deviations of 0.093% for RP-1 and 0.14% for RP-2. The parameters for Eq. (7) are listed in Table 8 together with their standard deviations which are much smaller than the parameter values indicating that they are statistically significant. The parameters for Eq. (8) are listed in Table 9, and their standard deviations are much larger than the parameter values, indicating that they are statistically not significant, as five adjustable parameters were determined by nonlinear least-squares regression from nine measured viscosity data for each sample. The parameters for Eq. (8) are given here nevertheless because this correlating equation is superior to Eq. (7) in its extrapolation behavior beyond the temperature range of the viscosity measurements. At temperatures below 293.15 K,

Eq. (8) yields increasingly higher viscosities than Eq. (7), with the difference reaching 10% at about 240 K. At temperatures above 373.15 K, Eq. (8) yields decreasingly lower viscosities than Eq. (7), with the difference reaching 10% near 480 K.

Conclusions

Density, speed of sound, and viscosity, along with data for the derived properties of adiabatic compressibility and isobaric thermal expansivity, have been presented for rocket propellants RP-1 and RP-2 over the combined temperature range from 270 to 470 K with pressures to 40 MPa. These data provide valuable information in the effort to formulate accurate equations of state for these fuels. For instance, the viscosity data accurately reflect the compositional differences between the two fuels. Additionally, the derived properties of adiabatic compressibility and isobaric thermal expansivity help us to further understand the chemical complexity of these fluids and give insight into possible advantages and or disadvantages of the chemical formulations of future rocket propellants. In this work, an emphasis was placed on enhancing the value of the data beyond the range in which they were measured by informed choices of correlations that yield physically meaningful results when extrapolated.

References

[1] Lemmon, E. W., Huber, M. L., and McLinden, M. O., "NIST Standard Reference Database 23: Reference Fluid Thermodynamic and Transport Properties-REFPROP," Vers. 8.0, National Inst. of Standards and Technology, Standard Reference Data Program, Gaithersburg, 2007.

[2] Andersen, P. C., and Bruno, T. J., "Thermal Decomposition Kinetics of RP-1 Rocket Propellant," *Industrial and Engineering Chemistry Research*, Vol. 44, No. 6, 2005, pp. 1670–1676.
doi:10.1021/ie048958g

[3] Bruno, T. J., and Smith, B. L., "Improvements in the Measurement of Distillation Curves. 2. Application to Aerospace/Aviation Fuels RP-1 and S-8," *Industrial and Engineering Chemistry Research*, Vol. 45, No. 12, 2006, pp. 4381–4388.
doi:10.1021/ie051394b

[4] "NIST Chemistry WebBook," *NIST Standard Reference Database Number 69* [online database], http://WebBook.NIST.gov [retrieved 2009].

[5] Ott, L. S., Hadler, A. H., and Bruno, T. J., "Variability of the Rocket Propellants RP-1, RP-2 and TS-5: Application of a Composition and Enthalpy Explicit Distillation Curve Method," *Industrial and Engineering Chemistry Research*, Vol. 47, No. 23, pp. 9225–9233.
doi:10.1021/ie800988u

[6] Laesecke, A., Outcalt, S., and Brumback, K., "Density and Speed of Sound Measurements of Methyl- and Propylcyclohexane," *Energy and Fuels*, Vol. 22, No. 4, 2008, pp. 2629–2636.
doi:10.1021/ef800049h

[7] Outcalt, S. L., and McLinden, M. O., "Automated Densimeter for the Rapid Characterization of Industrial Fluids," *Industrial and Engineering Chemistry Research*, Vol. 46, No. 24, 2007, pp. 8264–8269.
doi:10.1021/ie070791e

[8] Taylor, B. N., and Kuyatt, C. E., "Guidelines for Evaluating and Expressing the Uncertainty of NIST Measurement Results," National Inst. of Standards and Technology TN 1297, Washington, D. C., 1994.

[9] "Standard Test Method for Kinematic Viscosity of Transparent and Opaque Liquids (and the Calculation of Dynamic Viscosity)," ASTM International, Standard D445, West Conshohocken, PA, 2006.

[10] "Standard Specifications and Operating Instructions for Glass Capillary Kinematic Viscometers," ASTM International, Standard D446, West Conshohocken, PA, 2006.

[11] "Standard Test Method for Basic Calibration of Master Viscometers and Viscosity Oil Standards," ASTM International, Standard D2162, West

Table 8   Parameters of the viscosity correlations, Eq. (7), for the viscosity of RP-1 and RP-2 at ambient atmospheric pressure and temperatures from 293.15 to 373.15 K

Equation	*RP-1 sample*		*RP-2 sample*	
Parameter	Value	Standard deviation	Value	Standard deviation
β_{11}	2.17038	0.042	2.27186	0.081
β_{12}	0.424087	$7.3 \cdot 10^{-3}$	0.409842	0.014
β_{13}	−2.56715	0.028	−2.60843	0.056
AAD, %	——	0.091	——	0.18
RMS, %	——	0.104	——	0.19

Table 9   Parameters of the viscosity correlations, Eq. (8), for the viscosity of RP-1 and RP-2 at ambient atmospheric pressure and temperatures from 293.15 to 373.15 K

Equation	*RP-1 sample*		*RP-2 sample*	
Parameter	Value	Standard deviation	Value	Standard deviation
β_{14}	2.55848	$8.3 \cdot 10^3$	21.8278	$4.4 \cdot 10^4$
β_{15}	−3.505197	$1.2 \cdot 10^4$	−37.4932	$1.1 \cdot 10^5$
β_{16}	−3.41204	$4.6 \cdot 10^3$	−13.4044	$1.9 \cdot 10^4$
β_{17}	2.15509	$3.5 \cdot 10^3$	16.9258	$6.8 \cdot 10^4$
β_{18}	−3.145151	$1.7 \cdot 10^3$	−1.82885	$1.9 \cdot 10^3$
AAD, %	——	0.076	——	0.13
RMS, %	——	0.093	——	0.14

Conshohocken, PA, 2006.

[12] Petroleum products—Transparent and Opaque Liquids—Determination of Kinematic Viscosity and Calculation of Dynamic Viscosity, International Standards Organization, Standard 3104, Geneva, Switzerland, Oct. 6, 1994.

[13] Glass Capillary Kinematic Viscometers—Specifications and Operating Instructions, International Standards Organization, Standard 3105, Geneva, Switzerland, Jan. 12, 1994.

[14] Churchill, S. W., "The Art of Correlation," *Industrial and Engineering Chemistry Research*, Vol. 39, No. 6, 2000, pp. 1850–1877.
doi:10.1021/ie9908940

[15] Randzio, S. L., and Deiters, U. K., "Thermodynamic Testing of Equations of State of Dense Simple Liquids," *Berichte der Bunsen-Gesellschaft für Physikalische Chemie*, Vol. 99, No. 10, 1995, pp. 1179–1186.

[16] "Standard Test Method for Viscosity–Temperature Charts for Liquid Petroleum Products," ASTM International, Standard D341, West Conshohocken, PA.

[17] Brush, S. G., "Theories of Liquid Viscosity," *Chemical Reviews (Washington, DC)*, Vol. 62, 1962, pp. 513–548.

doi:10.1021/cr60220a002

[18] Vogel, H., "Das Temperaturabhängigkeitsgesetz der Viskosität von Flüssigkeiten," *Physikalische Zeitschrift*, Vol. 22, 1921, pp. 645–646.

[19] Fulcher, G. S., "Analysis of Recent Measurements of the Viscosity of Glasses," *Journal of the American Ceramic Society*, Vol. 8, No. 6, 1925, pp. 339–355.
doi:10.1111/j.1151-2916.1925.tb16731.x

[20] Tammann, G., and Hesse, W., "Die Abhängigkeit der Viskosität von der Temperatur bei unterkühlten Flüssigkeiten," *Zeitschrift für Anorganische und Allgemeine Chemie*, Vol. 156, 1926, pp. 245–257.

[21] DIPPR Project 801 Data Compilation of Pure Compound Properties, March 2007 ed., AIChE Design Inst. for Physical Properties, New York, 2007, http://DIPPR.BYU.edu.

[22] "ThermoData Engine Database," *NIST Standard Reference Database 103* [online database], Ver. 2.0, http://www.nist.gov/srd/WebGuide/nist103/103v2.htm [retrieved 2009].

C. Avedisian
Associate Editor